The effect of mechanical interactions between fibroblasts and epithelial cells in tumour initiation in a 3D collagen matrix

A Thesis submitted to

Indian Institute of Science Education and Research Pune in partial fulfilment of the requirements for the BS-MS Dual Degree Programme

by

R. Charvee

Indian Institute of Science Education and Research Pune

Dr. Homi Bhabha Road, Pashan, Pune 411008, INDIA.

April, 2020

Research Mentor: Prof. G.V.Shivashankar

Mechanobiology Institute, National University of Singapore

Singapore

CERTIFICATE

This is to certify that this dissertation entitled “TThe effect of mechanical interactions between fibroblasts and epithelial cells in tumour initiation in a 3D collagen matrix” towards the partial fulfilment of the BS-MS dual degree programme at the Indian Institute of Science Education and Research, Pune represents work carried out by R.Charvee at Mechanobiology Institute, National University of Singapore, Singapore under the supervision of Prof.G.V.Shivashankar, Professor, Mechanobiology Institute, National University of Singapore, SIngapore during the academic year 2019-2020,

Student
(R.Charvee)

Research Mentor
(Professor G.V.Shivashankar)

Committee:

Research Guide: Prof.G.V.Shivashankar

Expert Advisor: Dr. Kundan Sengupta

This thesis is dedicated to my Dad

for the years of encouragement and inspiration he offered me

DECLARATION

I hereby declare that the matter embodied in the report entitled “The effect of mechanical interactions between fibroblasts and epithelial cells in tumour initiation in a 3D collagen matrix” are the results of the work carried out by me at the Mechanobiology Institute, National University of Singapore, Singapore under the supervision of Prof.G.V.Shivashankar and the same has not been submitted elsewhere for any other degree.

R.Charvee

29.03.2020

TABLE OF CONTENTS

LIST OF FIGURES

ABSTRACT

Studies in the past few decades have shown that the precursor to cancer is not just a single heavily mutated cell but also the multiple cellular and acellular components of its microenvironment that contribute to its proliferation, progression and manifestation in other tissues. Tumour microenvironment is known to share multiple similarities with the microenvironment of a healing wound. However, the investigations on the ability of a wound-like situation leading to tumorigenesis in epithelial cells is not yet explored much. Several similarities in both the microenvironments have been reported, including exposure of epithelial cells to stromal fibroblasts and extracellular matrix, fibroblast recruitment and aggregation, enhanced fibroblast contractility as well as extracellular matrix remodeling. All these observations suggest the important role of mechanical microenvironment in both wound healing and tumor initiation. Fibroblasts play an important role in regulating the mechanical microenvironment in both the conditions. Therefore it is worth exploring the role fibroblast driven mechanical cues in tumour initiation in a wound-like environment. In this thesis, I have established a co-culture 3D collagen model in which fibroblasts and epithelial cells mechanically interact with each other. My hypothesis is that, due to the physical interaction fibroblasts pull epithelial cells through the constricted pore of collagen matrix, which may induce DNA damage in the epithelial cells that may lead to tumour initiation. In the course of my masters' thesis, I show that the epithelial cells and nucleus appeared to be elongated morphologies when they are pulled by the more contractile fibroblasts and aggregate of fibroblasts in a 3D co-culture model. Moreover, the enhanced DNA damage in these pulled epithelial nuclei validates our hypothesis as well as highlighting the potential role of mechanical cues in the tumour initiation.

ACKNOWLEDGEMENTS

The completion of this thesis could not be possible without the generous input of a number of people, and I'd like to take this opportunity to thank them.

Firstly, a big thank you to my guide Prof. G V Shivashankar, for the opportunity and guidance. It goes without saying that without him there would be no thesis.

Next, the lab group of Prof Shivashankar, who made me feel at home in a foreign country, and whose support got me through my time there. I would like to particularly mention Dr. Bibhas Roy, who invested a lot of time and effort in helping me in this project. Thank you so much!

Thanks also to the place I called home for these past months - the Mechanobiology Institute, National University of Singapore for funding my project, my stay and most of all, for being very generous hosts.

At the same time, I cannot forget my home institute - IISER Pune. Thanks to the academic office, MS-thesis committee and administration for their constant support.

My expert advisor Dr Kundan Sengupta, who went above and beyond to provide support and comfortable space in his lab post returning to India, thank you so much!

A special shout-out to my batchmate Dyuthi Sreekumar, whose company helped me battle homesickness in Singapore.

Thanks also to my senior Rahul Iyer for last minute valuable edits to this thesis.

1

INTRODUCTION

1.1 Cancer and tumor microenvironment

Characteristics of tumor microenvironment

Cancer is a complex disease that initiates with the uncontrolled proliferation of a few or a single transformed cell leading to a tumor mass. This, then, with the help of the other untransformed stromal cells, extracellular matrix (ECM), extensive network of blood vessels and other components of the tumor microenvironment, undergoes metastasis and establishes itself in other organs (Foster et al., 2018). As described by Robert Weinberg, the hallmark characteristics of cancer are: maintaining constant proliferative signalling, disabling mechanisms which suppress growth or promote apoptosis, vascularization and promoting invasion and metastasis of the transformed cells into other tissues. DNA damage and inflammatory responses can enhance the chance of getting these multitude of events to occur and hence promote cancer (Hanahan and Weinberg, 2000, 2011).

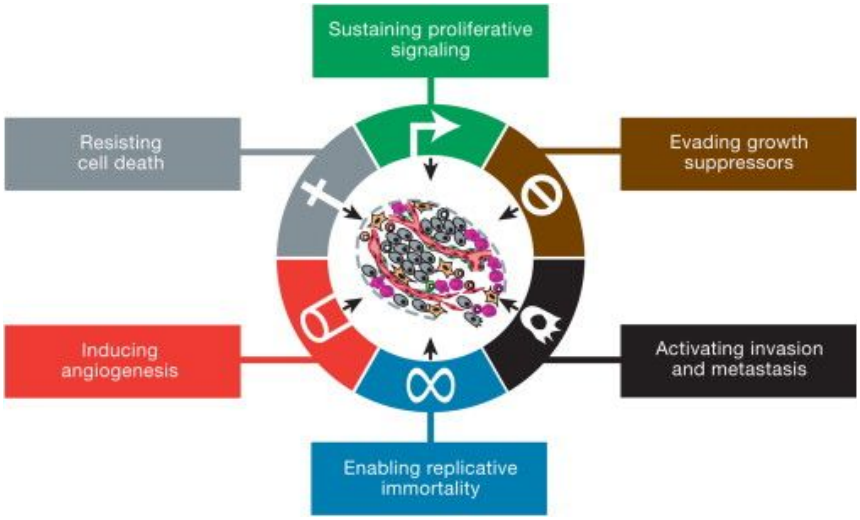

Figure 1.1: **Hallmarks of cancer:** (Hanahan and Weinberg, 2000, 2011).

Mechanical interactions in tumor microenvironment

The tumor microenvironment interacts with the tumor mass both biochemically as well as mechanically. In the mechanical space, the tumor mass is known to recruit the surrounding stromal fibroblasts and activate them, becoming Cancer Activated Fibroblasts or CAFs. CAFs are more contractile and deposit more Collagen-I as compared to normal stromal fibroblasts, hence making the tumor tissue matrix stiffer. Studies also show that CAFs form heterotypic N-cadherin and E-Cadherin junctions with the transformed cells (which in 90% of the cancers are of epithelial origin) and pull them away from the tumor mass in order to aid in their metastasis (Labernadie et al., 2017). Interestingly, both the mechanical aspects of tumor microenvironment - denser matrix and activated fibroblasts are also a characteristic of the microenvironment of a healing wound.

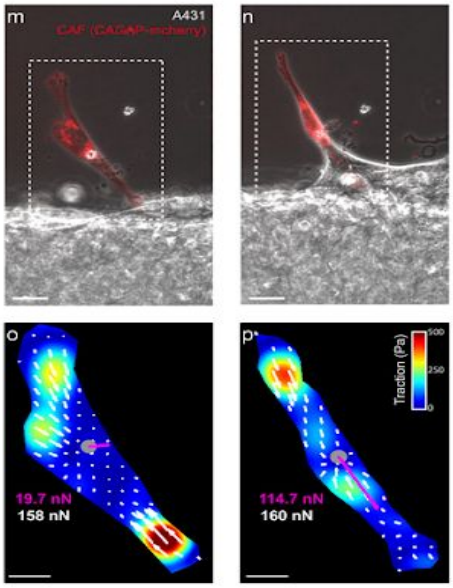

Figure 1.2: **Fibroblast driven migration of epithelial cells** (Left top): CAFs (red) before pulling the A431 cells and (Right top): CAFs after pulling the A431 cells. The bottom images show the traction force maps showing force generated by the CAFs while pulling the A431 cells. (Labernadie et al. 2017).

1.2 Cancer: a wound that does not heal

Wound microenvironment

A wound is established when the protective epithelial layer and basement membrane are ruptured. Wound healing starts with the clotting of blood, the components of which (fibrin, fibronectin, etc.) help in recruiting surrounding fibroblasts to the site of the wound (Peter Kujath, 2008). These fibroblasts then release inflammatory signals which then recruit immune cells which activate inflammatory response, in turn leading to activation of these fibroblasts. The activated fibroblasts deposit ECM proteins to fill in the matrix in the discontinuous tissue. The activated fibroblasts and the immune cells induce temporary epithelial to mesenchymal transition in the epithelial cells proximal to the wound leading to wound closure. And the deposited matrix appears as a scar after the wound heals.

Similarities between tumor microenvironment and wound microenvironment

Cancer is very often called a wound that does not heal. Tumour microenvironment shares multiple similarities with a wound microenvironment. For example, epithelial-mesenchymal transition (EMT) observed in epithelial cells during wound closure resembles EMT transition in transformed epithelial cells during metastasis. The other similarities include: activation of surrounding fibroblasts, fibroblast aggregation, collagen deposition by fibroblasts, extracellular matrix remodelling. In short, the Epithelial-Fibroblast-ECM interaction is widely similar in both the environments. Although studies have explored the similarities between these two physiological conditions to a large extent, there is less insight into exploring the possibility of a wound-like microenvironment promoting tumorigenicity in an otherwise normal epithelial cell (Foster et al., 2018).

Few evidences for wound-like environment predisposing normal cells to become tumorigenic

One such study indicated the possible role of wound-like environment in neoplastic transformation of otherwise normal cells in ovarian cancers. Epithelial Ovarian cancer is one of the more frequent cancers amongst women and 90% of ovarian cancers originate from Ovarian Surface Epithelium (OSEs). Studies show that post ovulatory repair process, which involves closure of wound by EMT of the OSEs also leads to rupture of the tunica albuginea, which separates the OSEs from the stromal matrix and cells. Post-ovulation, when the OSEs layer ruptures, some of the cells undergo EMT and migrate to close the wound, in this process, some OSE cells invaginate into the matrix and form certain inclusion cysts and are more prone to neoplastic transformation (Nicholas B Berry, 2008). Reports of DNA damage is also reported in these epithelial cells upon ovulatory rupture of OSE layer, which might enable tumorigenesis. While most studies following this focus on the biochemical aspects of wounds where inflammatory signals and oxidative stress are seen as the major causative factors of such transformation, very little focus has been placed on the mechanical effect of such conditions which may predispose the normal epithelial cells to undergo transformation (Murdoch et al., 2001).

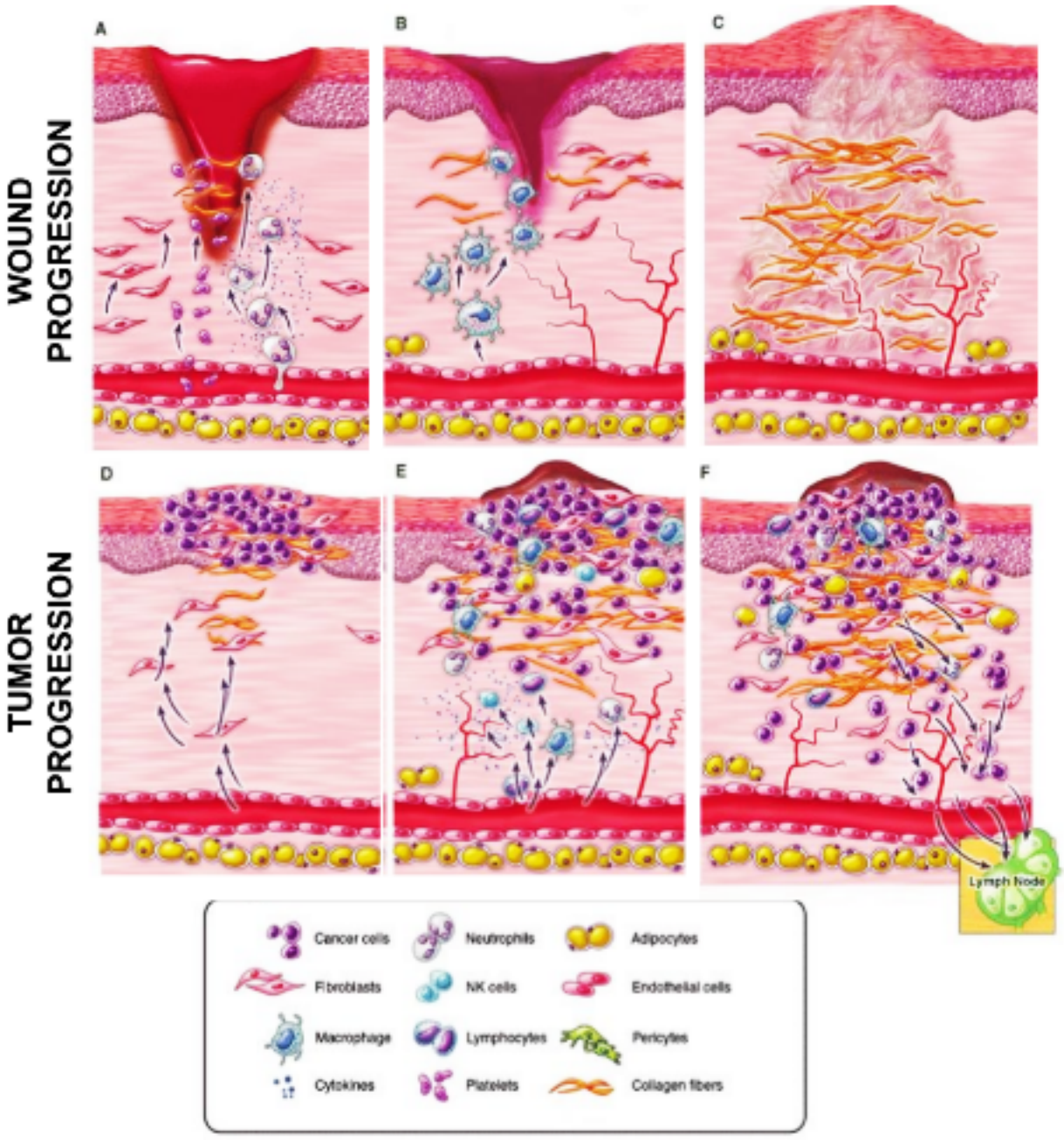

Figure 1.3: **Similarities between wound and tumour microenvironment: (**A-C) represents progression of events in wound healing starting from disruption of basement membrane. (D-F) represents events in tumour progression starting from hyper-proliferative tumor mass eventually leading to cancer.
(Foster et al., 2018)

1.3 Mechanical aspect of wound promoting tumorigenicity

Tumor promoting characteristics in a wound

As compared to healthy tissue, during a wound, the basement membrane separating the epithelial cells and the stromal layers rupture, exposing the epithelial cells to the ECM and stromal cells like the fibroblasts, macrophages, etc. Fibroblasts are recruited to the site of the wound, where they aggregate to help in wound closure by inducing EMT in epithelial cells and by depositing and remodelling Extracellular Matrix (ECM). These fibroblasts are known to become more contractile. As mentioned earlier, certain kinds of activated fibroblasts show the ability to pull cancer cells of epithelial origin. We wondered if the activated fibroblasts in a wound could pull the normal epithelial cells that come in contact with them through the dense ECM of the wound microenvironment. Denser matrices have smaller pore size. Studies show that stiffer tissues are likely to undergo more neoplastic transformations and face increased risk of tumorigenesis. Although mechanical stress induced proliferation and stiffness induced migration are contributing factors, it's suggested that DNA damage in the cells due to shear stress in the nuclei made to move through much smaller pores could also be another factor. Yet there have been no studies so far proving this in the 3D culture system with collagen matrices.

Studies using transwell assays show that when cells migrate through pores of size much smaller than the diameter of their nuclei, they undergo DNA damage (visualized by number of gH2Ax foci) and have mislocalized DNA repair proteins (Irianto et al., 2017). Hence in the wound-like environment, when the activated fibroblasts pull the epithelial cell through the stiff extracellular matrix, the nuclear envelope of the epithelial cell may be liable to rupture further leading to damage of the DNA within the nuclei. This may lead to neoplastic transformation of the epithelial cells.

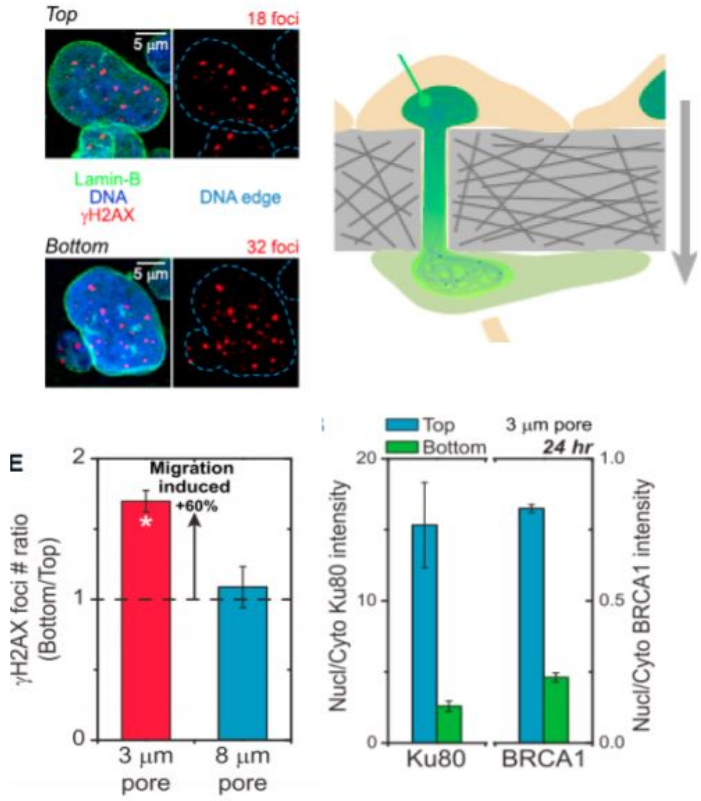

Figure 1.4: **DNA damage as a cancer cell migrates through a smaller pore** (3μm) as compared to (8 μm) is accompanied by mislocalized repair factors (Irianto et al., 2017).

The mechanical factors we believe will be responsible for increased tumorigenicity:

[a] Fibroblasts are known to be recruited at the site of wound and aggregate there.

[b] Fibroblasts are known to be activated (increased contractility) at the site of wound.

[c] Fibroblasts deposit and remodel Collagen-I at the site of wound.

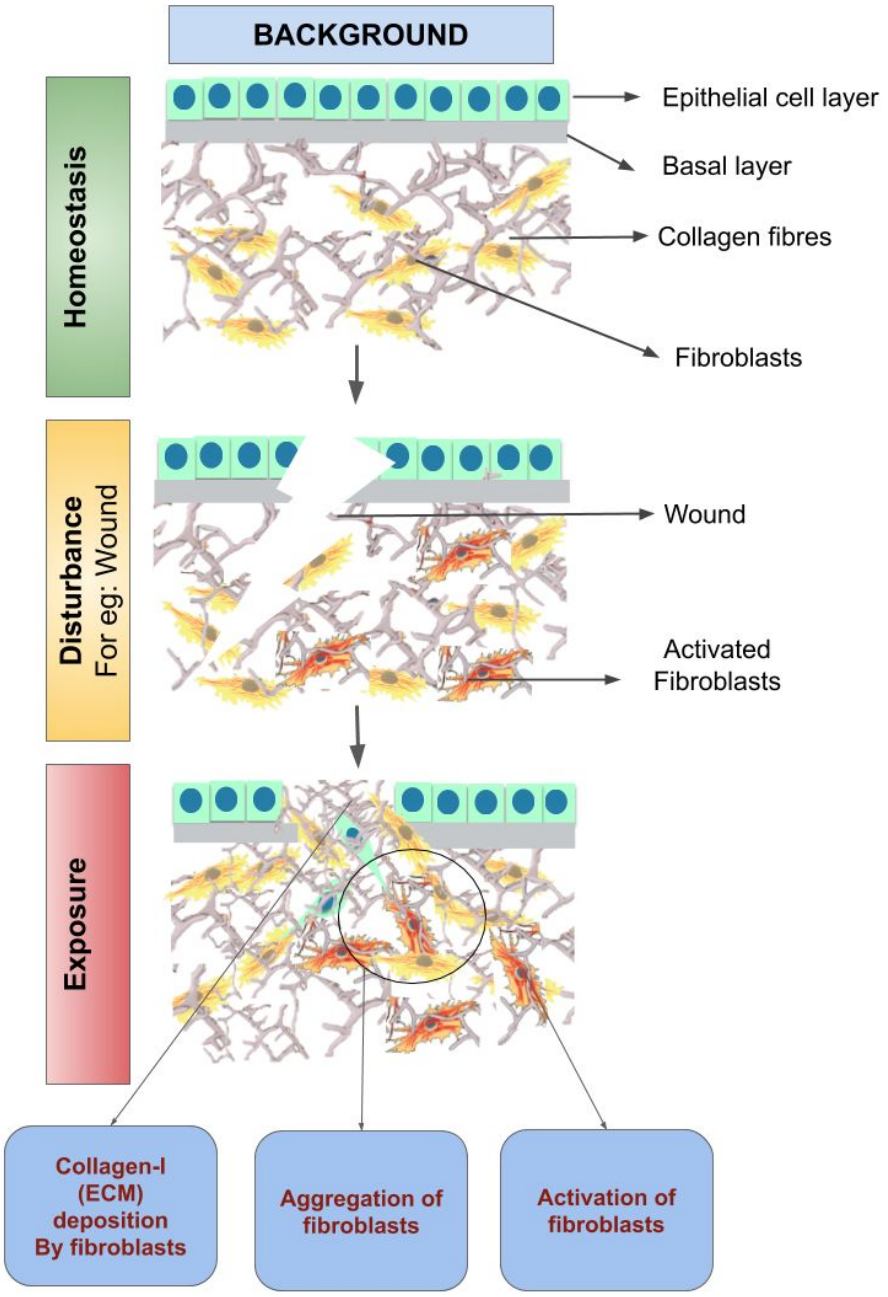

Figure 1.5: **Schematic depicting the mechanical interactions in wounds** relevant to exploring when studying their tumorigenicity.

1.4 Hypothesis

Our hypothesis is that during fibroblast driven migration, epithelial cells are pulled through the matrix pores much smaller than the diameter of their nucleus and thus DNA that is packaged into this nucleus is prone to get damaged and such continuous accumulations of DNA damage may lead to oncogenic transformation. In this paradigm, we wanted to investigate three questions:

(1) Whether fibroblasts derived from aggregates are comparatively more efficient to pull and deform epithelial cells in a 3D collagen matrix than singlets of fibroblasts?
(2) Whether enhanced contractile fibroblasts derived from reprogramming and redifferentiation are even more efficient to pull and deform epithelial cells?
(3) Fibroblast mediated migration of epithelial cells through the constricted pores of 3D collagen matrices whether they induce more DNA damage, which can lead to tumour initiation.

By investigating these mechanical aspects of the wound for their tumorigenic ability, we hope to uncover other possible mechanisms of initiating tumor apart from the existing mechanisms like carcinogen exposure, biochemical signalling induced DNA damage, etc. And in light of its success, traditional methods of treating wound or suppressing or activating processes in wound healing may come in handy to prevent wound-initiated-cancer in internal tissues. In order to study the tumour initiation process we established a in vitro 3D wound model by co-culturing human mammary epithelial (HME-I) cells and human mammary fibroblast (HMF-3A) cells in a 3D collagen matrix, which some extent mimicking the mammary model.

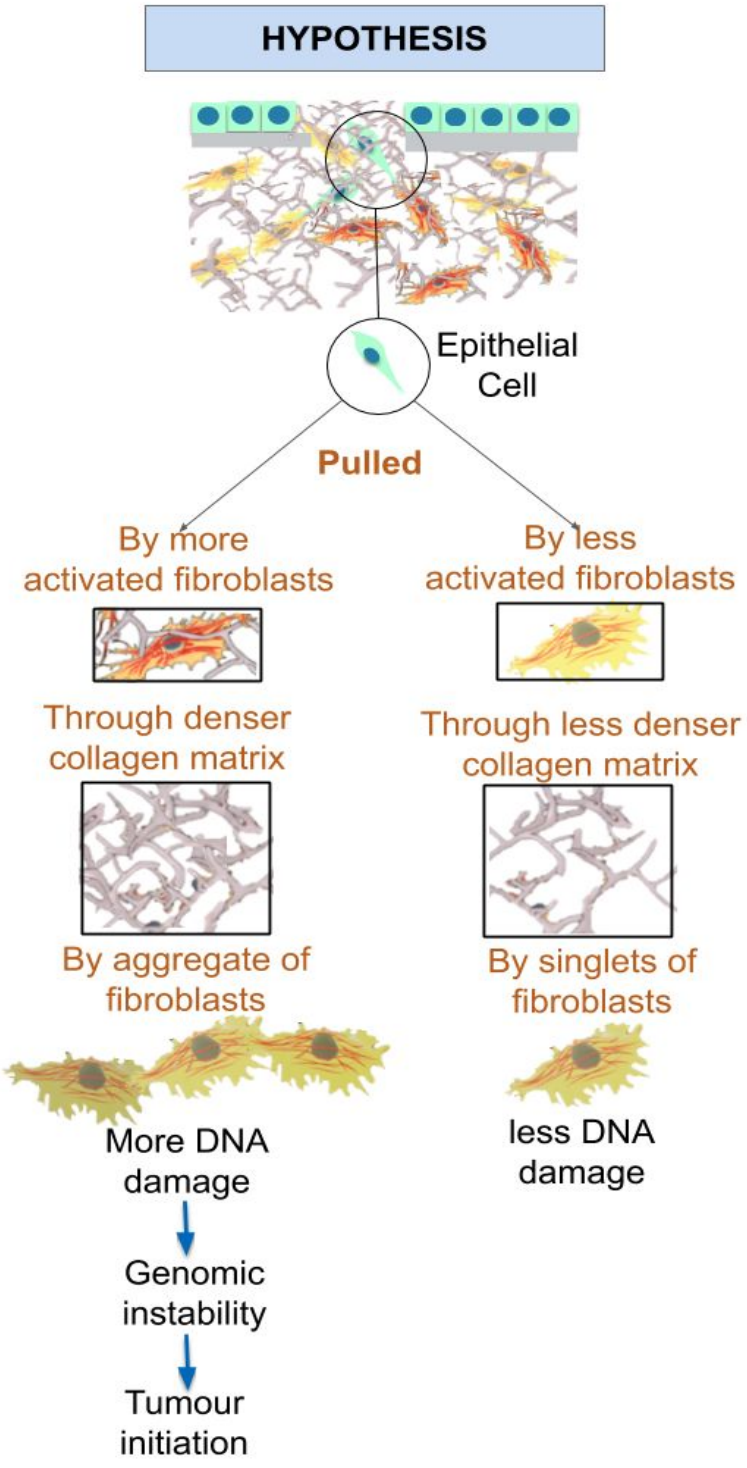

Figure 1.6: **Schematic depicting the hypothesis**

Objectives:

1. Designing a stable 3D co-culture model to study mechanical interactions between HME-I epithelial and HMF3A fibroblasts cells by
    a. Generating enhanced contractile HMF3A using partial reprogramming and redifferentiation.
    b. Optimizing the culture conditions for the HMF3A and HME-I co-culture.
    c. Establishing a stable collagen matrix based 3D co-culture model to study role of mechanical cues in tumour initiation.

2. To establish that HME-I is indeed pulled by HMF3A cells when co-cultured by comparing HME-I nuclear elongation in co-culture as compared to control HME-I

3. Aggregate vs Singlet fibroblasts: Compare the effect on HME-I when pulled by fibroblasts derived from aggregate of HMF3A as against by singlets of HMF3A. Measure the HME-I nuclear elongation and DNA damage.

4. More contractile vs Less contractile fibroblasts: Compare the effect on HME-I when pulled by more contractile HMF3A (generated by partial reprogramming and redifferentiation of normal HMF3A cells) against less contractile HMF3A. Measure the HME-I nuclear elongation and DNA damage.

2

MATERIALS AND METHODS

2.1 Partial reprogramming of fibroblasts and redifferentiation

Human Mammary Fibroblasts (HMF3A) were cultured on fibronectin micropatterns and grown under laterally confined conditions. For this, rectangular micropatterns of 3300 μm^2 area and 1:4 aspect ratio were printed on uncoated Ibidi dishes (81151) by stamping fibronectin (F1141, Sigma) coated PDMS micropillars. Following this, the surface of the micropatterned dish was passivated with 0.2% pluronic acid (Sigma P2443) for 10 min. HMF3A cells were expanded in high-glucose DMEM (Gibco) + 10% (vol/vol) FBS (Gibco) and 1% penicillin-streptomycin (Gibco) and at 37^0 C. For partial reprogramming, HMF3A cells were seeded on these fibronectin-micropatterned dish at a concentration of ~7,000 cells in 1.5mL of media per dish to achieve a cell density of one cell per fibronectin island. Single cells were grown under laterally confined conditions for 8 days in the above mentioned culture medium. In control HMF3A clump conditions (FC), similar spheroid size and cell density (compared to 6-day partially reprogrammed spheroids) was achieved by seeding HMF3A cells on the similarly micropatterned dishes at a concentration of ~80,000 cells per dish and growing them overnight. For redifferentiation, spheroids were embedded in 3D rat tail Collagen-I gel of 1mg/mL concentration according to the manufacturer's protocol (Thermofisher). In such a 3D collagen matrix, cells were cultured for 48h in the above mentioned medium for most of the rejuvenation assays unless otherwise stated.

2.2 Co-culturing of epithelial cells and fibroblasts cells:

Human Mammary Epithelial cells (HME-I) were expanded in MEGM (Lonza). Co-culture experiments with HME-I and HMF-3A cells were done in medium containing the above

mentioned HMF3A culture medium and HME-I culture medium in 1:1 ratio. Before mixing the two different cell lines, the HME-I cells were coloured with cell cytoTracker (488 nm) for ease of differentiating the cell lines during imaging and image analysis. For the Wound Model of co-culture, HME-I were seeded in uncoated ibidi dishes (81151) at a concentration of ~1,000,000 cells per dish and cultured for 2 days. Following this, clean scratches were made with a sterile 1mL pipette tip. The HMF3A PR spheroid/ HMF3A clumps were deposited in a low volume (~40-50µL) only near the scratched area and incubated at 37^0 C for 30-40 mins. After this, they were embedded in 1mg/ml collagen matrix and cultured for two days. For the Clump Model of co-culture, HME-I cells were seeded at a concentration of ~80,000 cells per dish on uncoated ibidi dishes (81151) which were micropatterned similar to the procedure mentioned before and cultured for two days. To this, HMF3A PR spheroids/HMF3A clumps were deposited in low volume (~40-50µL) close to the areas of HME-I clump formation and incubated for 37^0 C for 30-40 mins. After this, they were embedded in 1mg/ml collagen matrix and cultured for two days.

2.3 Immunostaining

Fixation of cells embedded in Collagen-I gel was done with 4% Paraformaldehyde (Sigma) in PBS buffer (pH 7.4) for 30 min, followed by three washes with PBS + 100mM glycine buffer. Permeabilization of the cells was done using 0.8% Triton (Sigma-Aldrich) in PBS for 20 min, followed by three PBS-glycine buffer washes. Following this, cells were blocked using 10% goat serum (ThermoFisher Scientific) in IF wash buffer (PBS + 0.2% Triton + 0.2% tween 20) for 3h at room temperature. Cells were then incubated overnight with different primary antibodies diluted in a blocking buffer, followed by three 15 minute washes with IF wash buffer. Cells were then incubated with required fluorescent-labeled secondary antibodies diluted in 5% goat serum in IF wash buffer for 3h at room temperature. The nuclei of the cells were stained using NucBlue Live Ready Probes (Molecular Probes; Thermo Fisher Scientific) in PBS for 10 min at room temperature, and filamentous actin was labeled using phalloidin Alexa Fluor 647 (1:100;

Molecular Probes; Thermo Fisher Scientific) for 45 min.

2.4 Alkaline Phosphatase Assay

Cells were fixed with 4% Paraformaldehyde (Sigma) at room temperature for 30 min, followed by washing with PBS and Tris buffered saline (100 mM Tris and 5 mM $MgCl_2$ in deionized water). The cells were incubated with the alkaline phosphatase substrate 5-bromo-4-chloro-3-indolyl phosphate/nitro blue tetrazolium (BCIP/NBT) (Sigma-Aldrich) at room temperature under slowly rocking conditions. The pluripotent cells would stain pinkish blue-colored cells with time. To avoid oversaturation, plates were monitored under bright-field microscopy, and the reaction was stopped, as required, by aspirating the substrate solution and rinsing with PBS.

2.5 Image acquisition and analysis

Fluorescent images of 3D spheroids and cells embedded in 3D Collagen-I gel were acquired by using Nikon A1R laser scanning confocal microscope (Nikon Instruments Inc, Japan), at either 40x magnification or 60× magnification with identical acquisition settings. In the Z dimension, each spheroid and 3D Collagen-I gel was scanned up to a depth of 35 µm, with a step size of 1 to 2 µm. Confocal images of either 512x512 pixels were obtained with an XY optical resolution of 0.42 µm. The fluorescence intensity of each protein was measured in its corresponding channel and the gH2Ax foci per nucleus were determined using IMARIS8. To determine the nuclear sphericity of a subpopulation of cells within the co-culture, the nuclei were thresholded with mean intensity of the channel corresponding to the fluorescent marker selectively staining this subpopulation. This was done using IMARIS8.

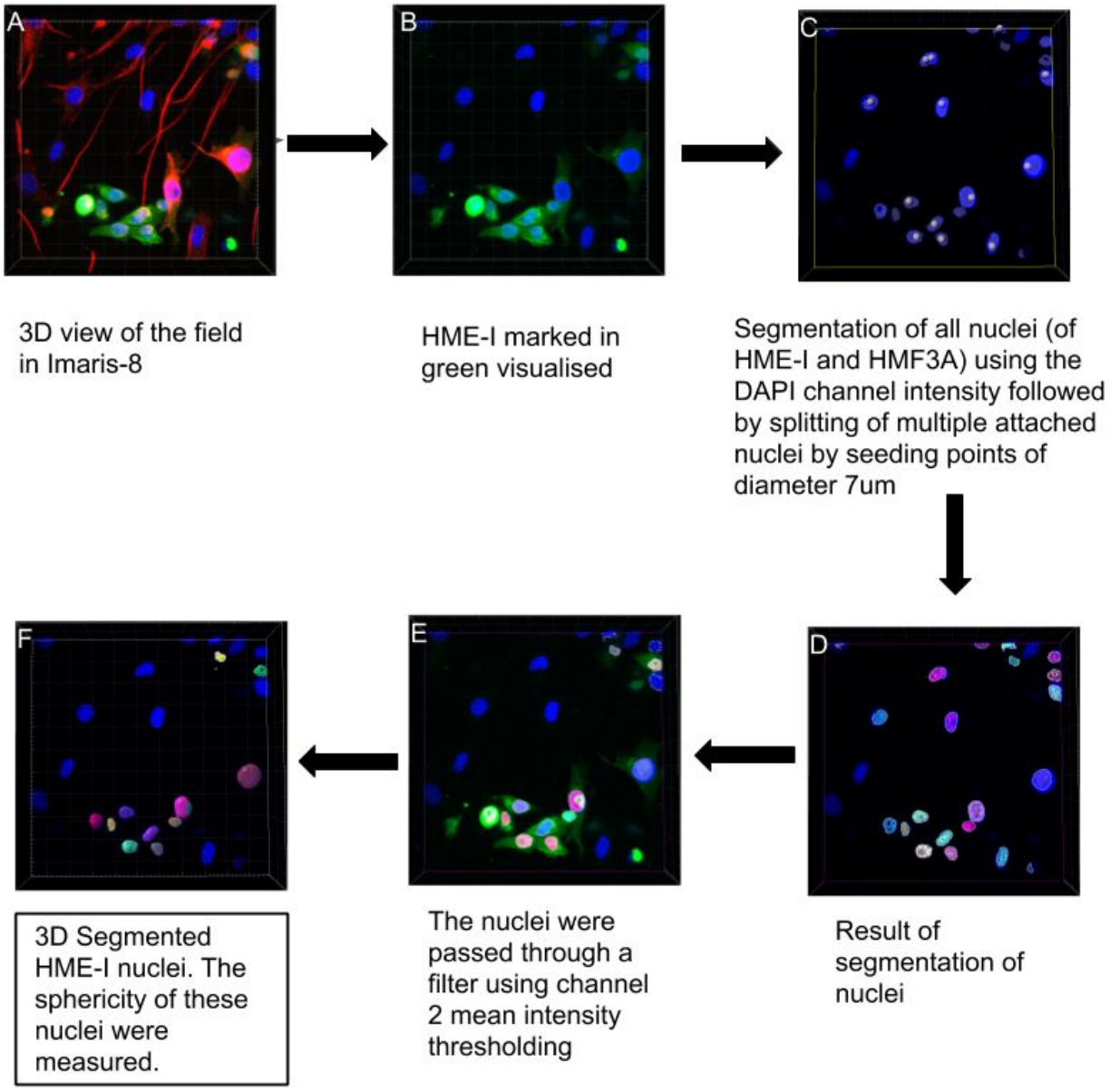

Figure 2.1 **HME-I Nucleus segmentation using IMARIS-8 to obtain sphericity values**

3

RESULTS AND DISCUSSION

3.1 Establishment of 3D co-culture model to study mechanical interaction between fibroblast, epithelial cells and ECM

3.1.1 Fibroblasts of enhanced contractility are obtained by a novel method of partial reprogramming followed by re-differentiation.

Our lab has shown earlier that when confined laterally on fibronectin micropatterns of appropriate dimensions, and allowed to grow for long enough, fibroblasts grow into pluripotent spheroids (Roy et al., 2018). In this state of transition from differentiated to reprogrammed cells, when they are embedded as partially reprogrammed spheroids in 3D collagen matrix of appropriate stiffness, they redifferentiate back into fibroblasts with enhanced contractility, as confirmed by cytoskeletal genes' expression profile and enhanced LaminA and acto-myosin contractility (Roy et al. PNAS 2020 - in press) (*Figure 3.1*). This was shown in NIH3T3 fibroblasts of a mouse cell line. In order to validate its applicability in Human Mammary Fibroblasts (HMF3A), we repeated the procedure using HMF3A cells.

Rectangular micropatterns of appropriate size were identified and HMF3A cells were grown on them in laterally confined condition for 10 days (*Fig.3.2A*) and were fixed at different time points to check for change in oct4 expression with time using immunostaining (*Fig.3.2B*). An increase in nuclear oct4 expression was observed with time, with 10d samples showing a higher oct4 nuclear mean intensity as compared to 8d and 6d (*Fig.3.2C*). The data has been analysed for only a single replicate as a

preliminary observation. For a detailed characterization of reprogramming in laterally confined HMF3A, please refer to the thesis of Dyuthi Sreekumar, 20151059.

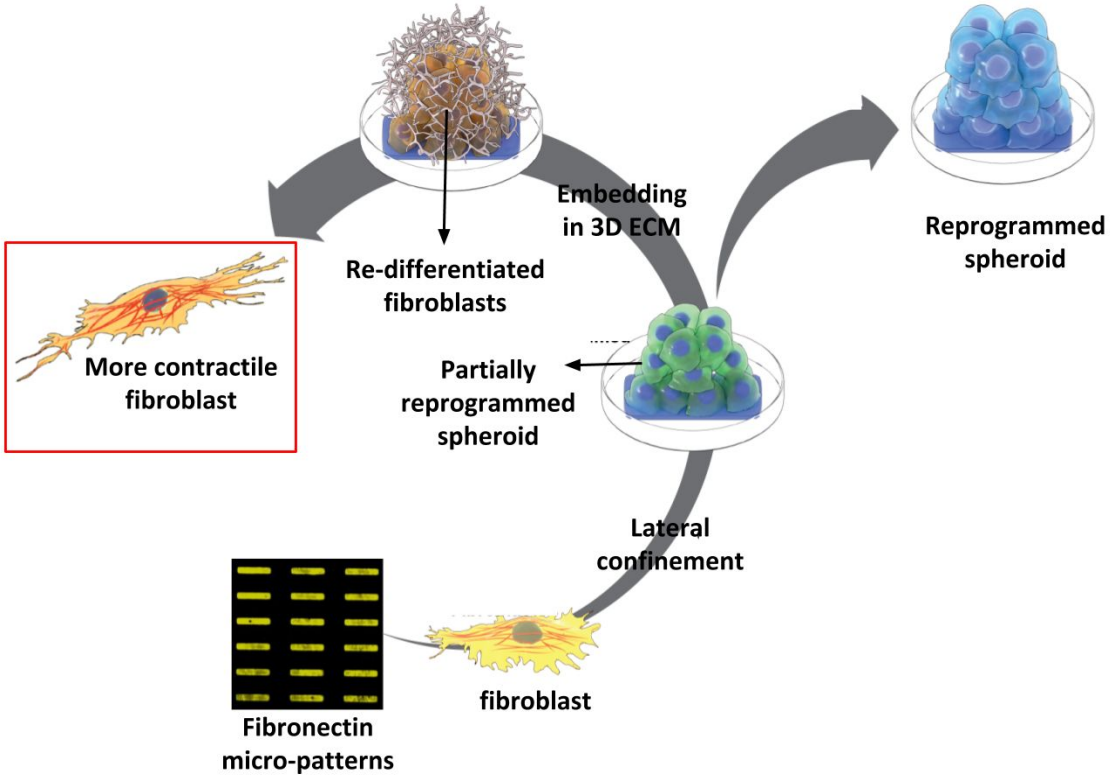

Figure 3.1: **Schematic for Novel method of generating more contractile fibroblasts**: laterally confined growth of fibroblasts on fibronectin micropatterns and embedding 3D ECM in a partially reprogrammed stage to become re-differentiated into fibroblasts of higher contractility. Adopted from *Roy et al. PNAS 2020 (in press)* and modified.

As a more confirmatory assay, we checked for alkaline phosphatase (AP) activity which is known to be up-regulated in pluripotent stem cells. In stem cells, where AP is higher, characteristic purple colouration is expected. As expected, the day 10 spheroids showed a higher AP activity as compared to the unpatterned surface cells grown upto 60% confluency with no lateral confinement and HMF3A clump controls *(Fig.3.2D,E)* and was found consistent across replicates (*Fig.3.2S)*. The difference in AP activity between 8 day and 10 day spheroids is not too significant, similar to the Oct4 read out.

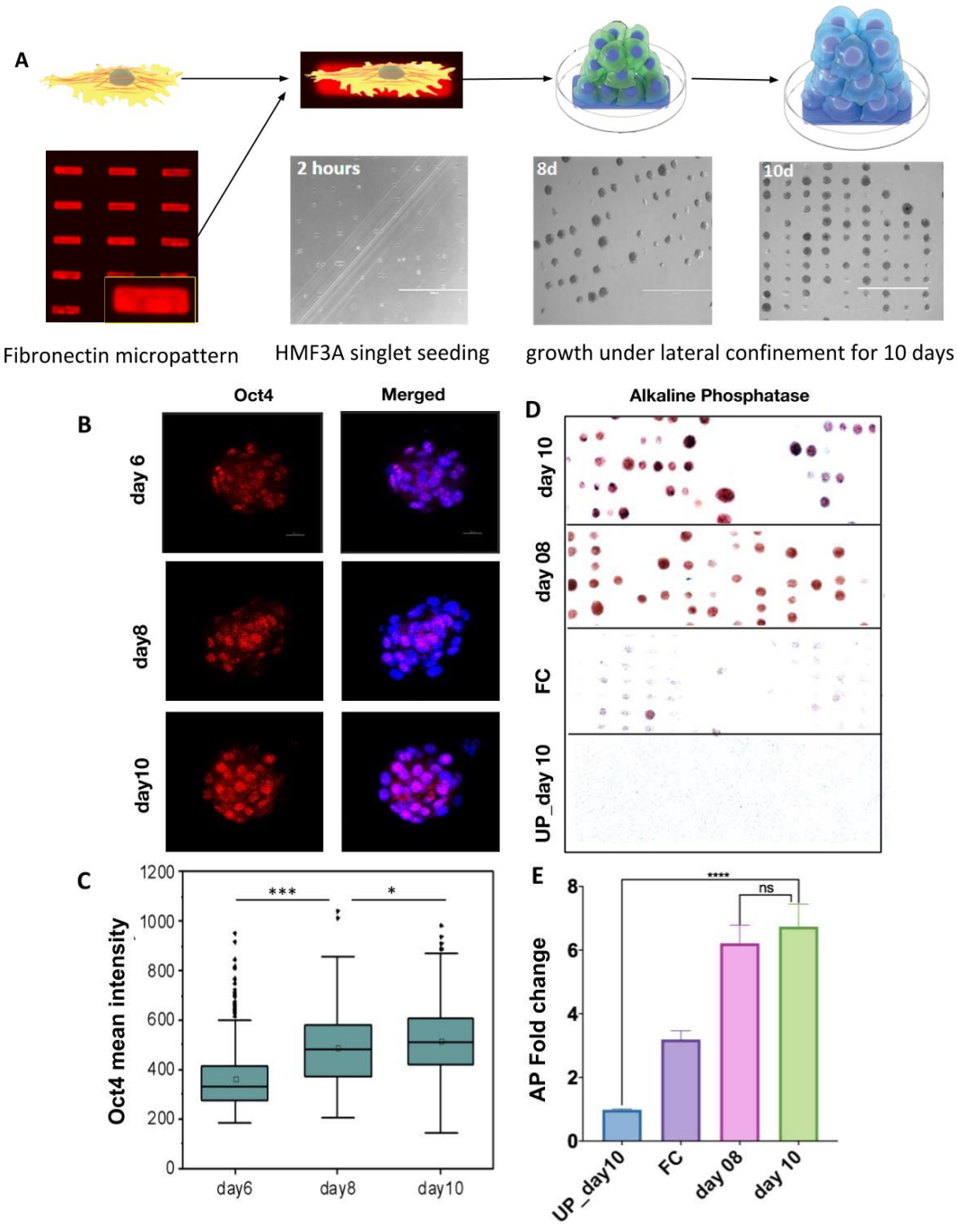

Figure 3.2: **Lateral confinement induced reprogramming of HMF3A: A**: (above) Schematic of the reprogramming process and (below) HMF3A cells cultured in laterally confinement on 3000 sq.µm rectangular fibronectin micropatterns for 10 days (scale bar=1000µm). **B:** Representative micrographs of HMF3A grown in lateral confinement for 6 days, 8 days and 10 days and immunostained for Oct4. **C:** Plot

of the Oct4 mean intensity per nucleus (au) for each condition (graph and analysis: student's t-test, ***P<0.001, *P<0.05, N=1, n=300, Median +/- SD). **D:** Alkaline Phosphatase (AP) activity, an indicator of stemness, in four different conditions- 10 days (day 10), 8 days (day 08) under lateral confinement; HMF3A clump (FC) and as Unpatterned cells grown without lateral confinement for 10 days (UP_ day10). **E:** Quantification of spheroid level fold change in Alkaline Phosphatase colouration in the above mentioned conditions (graph and analysis: N=3, n=75; Mean +/- SEM, students' t-test ****P<0.0001,ns-non-significant).

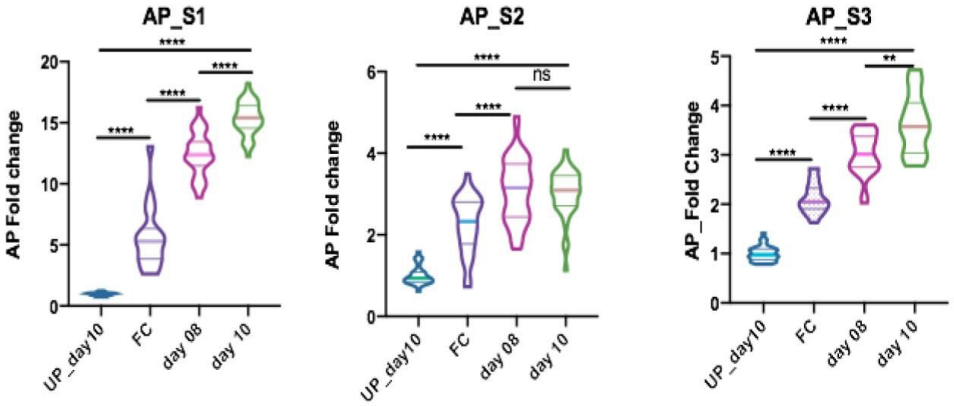

Figure 3.2S: Replicate data for Figure 3.2(E): A violin plot showing the fold change in alkaline phosphatase(AP) between conditions in three different replicate (graph and analysis: n~25, the width of the violin qualitatively represents the frequency of that observation, midline represents median with first and the third quartile, mann whitney t-test ns-non-significant, ****P<0.0001, **P<0.01)

We embedded partially reprogrammed HMF3A spheroids and HMF3A clump (refer *Materials and Methods*) in collagen matrix of 1 mg/ml concentration and cultured for two days, hereafter called Re-differentiated Fibroblasts (RF) and Fibroblasts Clump in Gel (FCG) respectively (*Figure 3.3A*). To check if the redifferentiated fibroblasts are more contractile in nature, we looked for the expression of pMLC and Actin (*Figure 3.3B*). As expected, the RF shows higher Actin cellular mean intensity as compared to the FCG*(Figure 3.3C)*, consistent across three biological replicates*(Figure 3.3S)*. While the pMLC shows considerable increase in RF as compared to FCG*(Figure 3.3C)*, this observation is limited to a single replicate*(Figure 3.3S)*. Although, the second replicate doesn't show a considerable increase. We henceforth used the fibroblasts thus obtained

(Redifferentiated Fibroblasts or RF) against the control fibroblasts (Fibroblasts Clump in Gel or FCG) to test our hypothesis that more contractile fibroblasts will pull the epithelial cells more and hence induce more DNA damage .

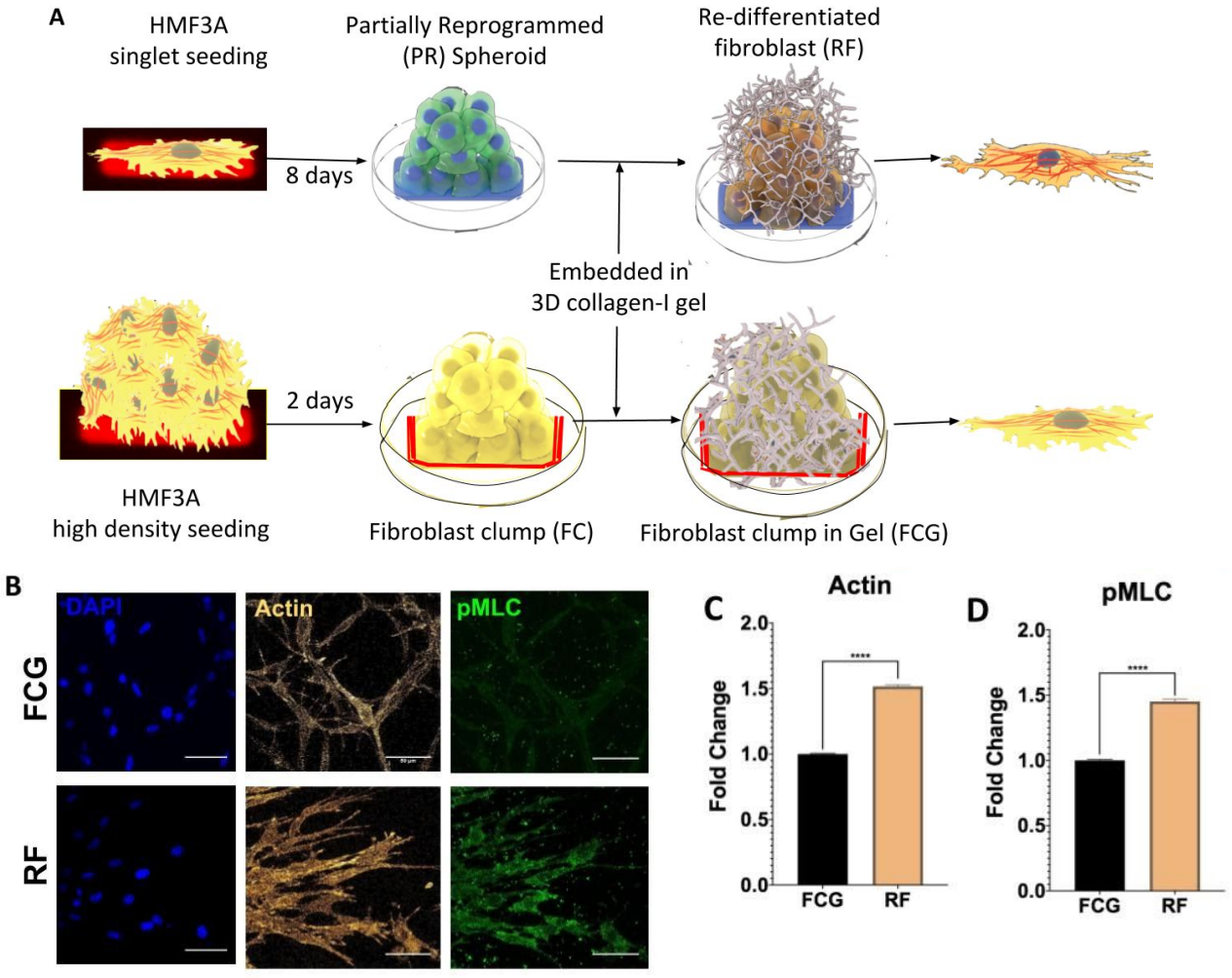

Figure 3.3: **Redifferentiation of partially reprogrammed HMF3A spheroids A:** Schematic of redifferentiation process for generating fibroblast of two different contractility by (above) embedding partially reprogrammed spheroids of HMF3A in 3D collagen matrix and (below) embedding clumps of HMF3A (FC) in 3D collagen matrix. **B**. Representative micrographs of Actin and pMLC immunostaining staining for Fibroblast Clump in GEL (FCG) and Re-differentiated Fibroblasts (RF) done to characterize their contractility (Scale bar: 50 μm) **C, D:** Quantification of Fold change in cellular mean intensity of Actin and pMLC respectively between FCG and RF. (graph and analysis: C: N=3,n=1500 Mean+/- SEM D: N=2, n=1000 Mean +/- SEM multiple t-test ****P<0.0001)

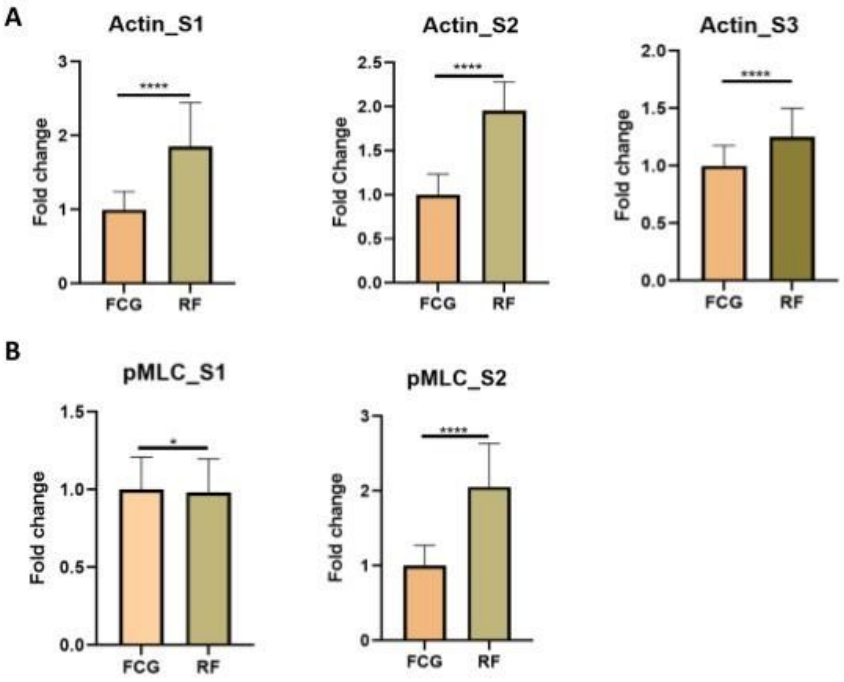

Figure 3.3S: **Replicate Data for Figure 3.3 (C,D)**: **A,B:** Box plot showing the fold change in cellular actin and pMLC respectively between FCG and RF, across multiple replicates (graph and analysis: n=500, mean +/- SD, mann whitney t-test ****P<0.0001, *P<0.05)

3.1.2 Optimizing the culture conditions for the HMF3A and HME-I co-culture.

We observed the growth of HMF3A cells and HME-I cells, cultured separately in three different media: a) HMF3A culture medium, b) HME-I culture medium and c) media comprising of HMF3A and HME-I culture medium in 1:1 composition (For details of cell specific culture medium please refer to *Materials and Methods*). While the HME-I cells showed poor growth in HMF3A culture media and HMF3A showed poor growth in HME-I culture media, an optimal growth in both cell types were observed in 1:1 growth medium. For the co-culture experiments thereon, we used HMF3A culture media: high-glucose DMEM(Gibco) + 10% (vol/vol) FBS (Gibco) and 1% penicillin-streptomycin (Gibco) and HME-I culture media: MEGM(Lonza) in 1:1 ratio.

3.1.3 3D co-culture model is established to study mechanical interactions between HME-I, HMF3A and Collagen-I.

We tried two different models to study the effect of mechanical interaction between the fibroblast and epithelial cells, namely Wound Model and Clump Model (*Figure 3.4A*) .

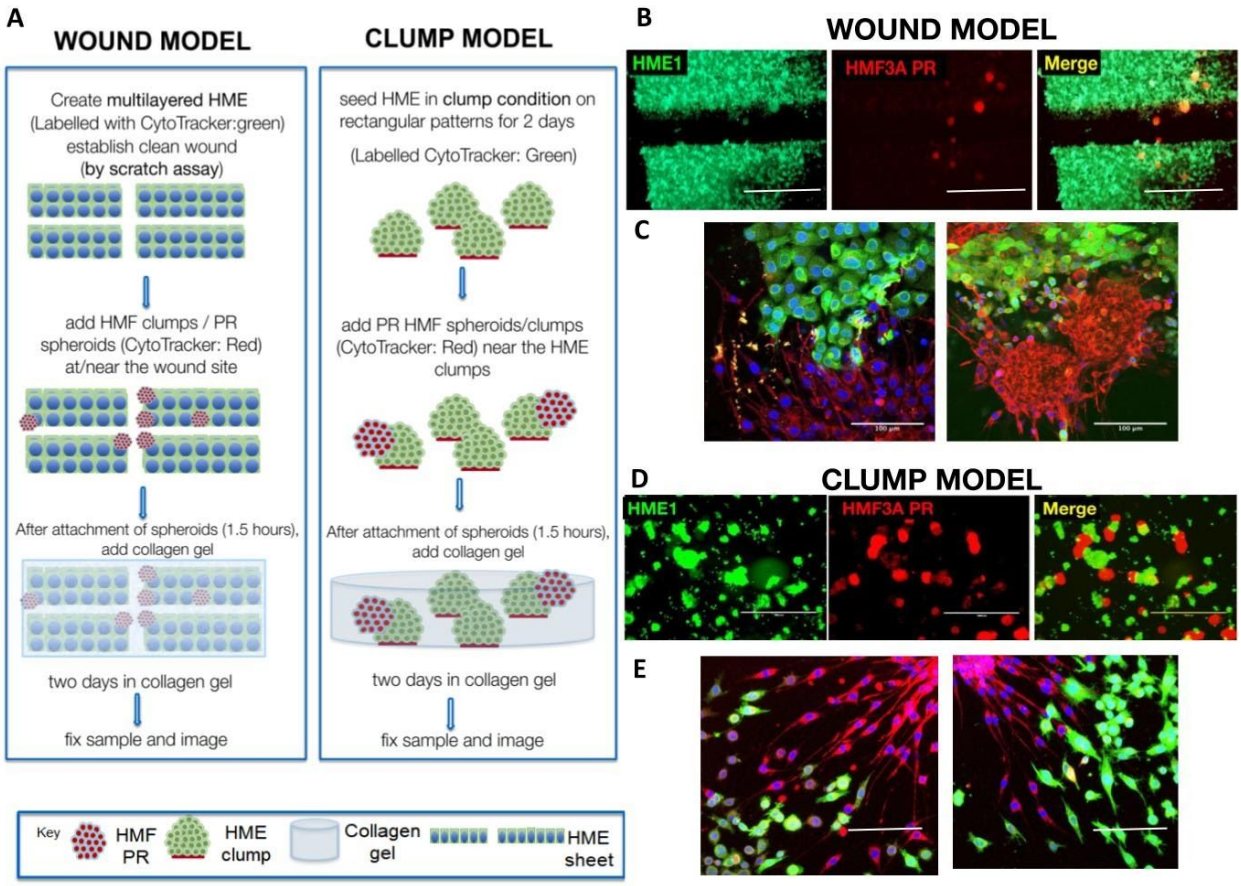

Figure 3.4: **3D co-culture models for studying mechanical interactions between fibroblasts and epithelial cells: A:** Schematic of two different models, the Wound Model and the Clump Model, showing how the model was established. **B,D:** Representative images of the wound model and the clump model respectively after adding the HMF3A PR spheroids and before embedding in collagen-I gel (Scale Bar: 2000 μm) where HME-I is stained with green cytotracker and HMF3A with red cytotracker. **C,E:** Representative micrographs of interaction between HMF3A cells and HME-I cells in the wound model and the clump model respectively after embedding in collagen-I gel for two days (Scale Bar: 100 μm).

Briefly, in the Wound Model, we made a scratch on a HME-I cell multilayer and deposited HMF3A Partially Reprogrammed spheroids close to the scratch (*Figure 3.4B*). Whereas in the Clump Model, we made clumps of HME-I cells by seeding them in high density on micropatterned dishes and then deposited HMF3A PR spheroids close to the clumps (*Figure 3.4D*).

After this, we embedded them on 1 mg/mL collagen matrix and cultured them for two days. We observed more elongated HME-I cells in the Clump Model which might be a result of either pulling or remodelling of the collagen matrix by the fibroblasts (*Figure 3.3C,E*). We didn't notice as many elongated cells in the Wound model. This could be because the layer of HME-I cells are strongly adhered to the bottom of the dish they were grown in. Hence a much larger force than the one exerted by the fibroblasts might be needed to pull them through the collagen gel. Noting all such shortcomings, the Clump Model was chosen for the further study of the mechanical interaction between HME-I and HMF3A cells.

3.2 HME1 cells show elongated morphology when co-cultured with HMF3A

3.2.1 HME-I show higher elongation co-cultured with fibroblasts derived from aggregates/clumps of HMF3A than HMF3A singlets

We wanted to first check if fibroblasts do indeed pull the epithelial cells through the collagen-I matrix, and if aggregate/clump of fibroblast have a higher pulling efficiency than singlets of fibroblasts. So we compared the 3D cellular and nuclear sphericity (which negatively correlates with their elongation) of the HME-I cells in various conditions- HME-I clump (**HME only**); HME-I clump co-cultured with singlets of HMF3A (**HME+S**); HME-I clump co-cultured with aggregate or clump of HMF3A (**HME+C**) all embedded in 3D collagen-I matrix for two days (*Figure 3.5A,B*).

The results show that the HME-I nuclear sphericity is lesser in the co-culture as compared to the control. Since pulling is a more local and possibly rare phenomenon and depends on how well fibroblast-epithelial cell contacts are established, comparing the average values over replicates was less helpful. So we calculated the fraction of cells/nuclei below a particular threshold sphericity within each condition . We noticed that there higher fraction of cells/nuclei below the threshold sphericity is present in co-culture as compared to the control. And a higher fraction of HME nuclei are below the threshold sphericity in case of HME+C as compared with HME +S (*Figure 3.5C,D,E,F*). Although the result comes to be insignificant upon doing statistical analysis, this could be because High inter-replicate variance in the fraction of cells elongated. Yet, each biological replicate shows a similar trend. And very interestingly, the minimum HME-I nuclear and cellular sphericity is clearly lesser in the case of HME+C as compared with HME+S in all the replicate data(*Figure 3.5S A,B*).

We suspect that this could be because, when incubated as clumps, HMF3As tend to form strong cell-cell contacts with each other, and upon embedding them in 3D collagen gel, they may emerge out from their clumps as a train of HMF3As rather than singlets. While this happens, the individual HMF3A contractility increases as it is in-turn pulled by a train of HMFs. When such an HMF3A cell pulls an HME-I cell, the force of pulling is likely to be higher. We suspect this may be the reason that a more elongated HME cell (with a lower cellular and nuclear sphericity) is observed in case of HME+C as compared with HME+S and further lower in the HMEonly. Interestingly when we compared the HMF3A nuclear elongation (Aspect Ratio), we observed that HMF3A in clumps are more elongated than HMF3A singlets, suggesting higher contractility(*Figure 3.5G*). The reason to believe that HMF3A has mechanical interaction with HME-I is because the HME-I cells in each field in HME+S and HME-C seem to be oriented with HMF3A nuclei in those fields (as shown in *Figure 3.5H* with three representative fields).

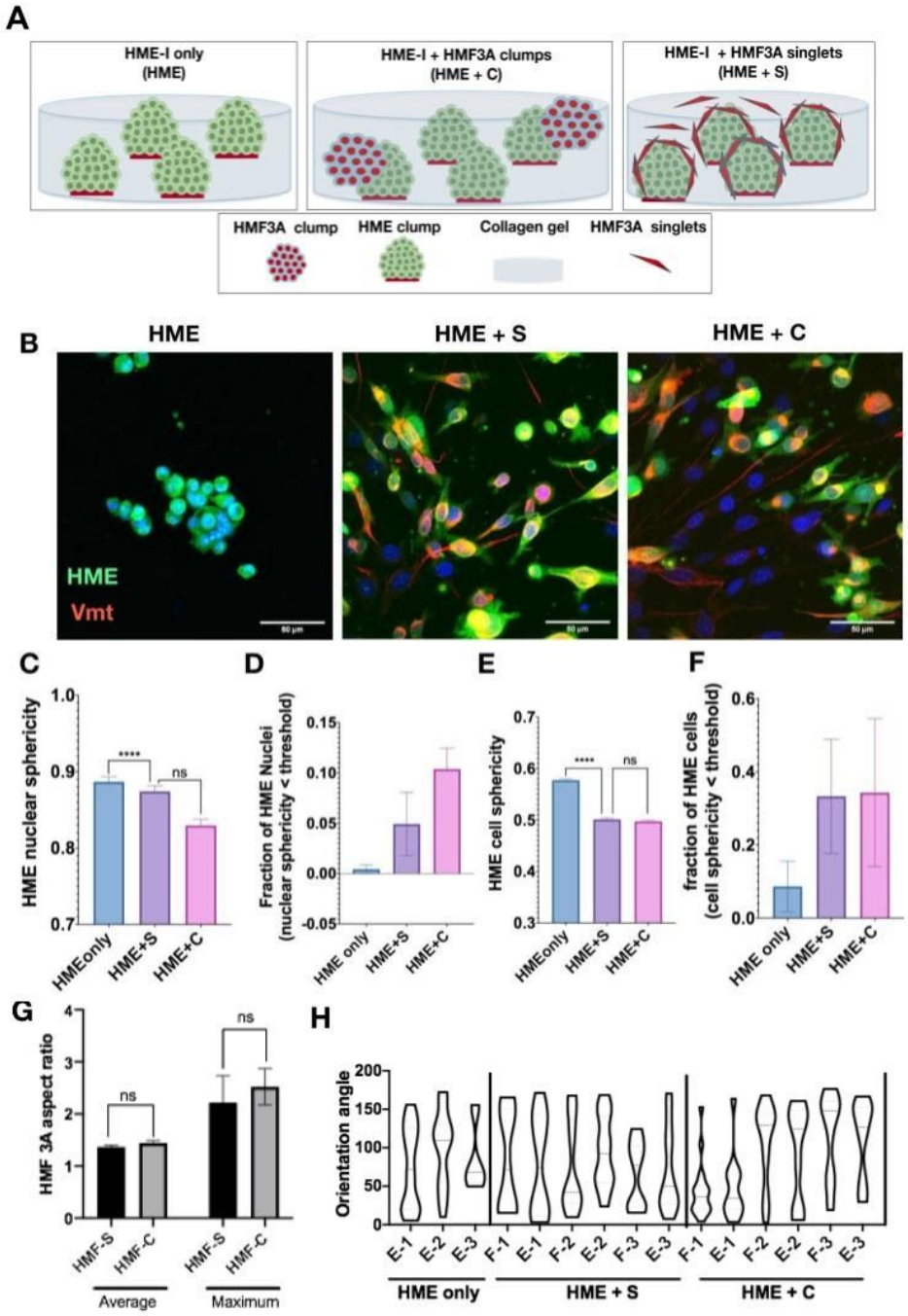

Figure 3.5: **Effect of pulling by aggregate vs singlets of fibroblasts: A:** Schematic representation of the different conditions in the experiment. **B:** Representative micrographs of HME-I clump (Left: HME-I), HME-I co-culture with singlets of HMF3A (Centre: HME-I+S) and HME-I co-culture with aggregates/clumps of HMF3A (Right: HME-I+C) after embedding in 3D collagen-I matrix for two days(Scale Bar = 50 μm). **C, E:** Bar graph comparing average HME-I nuclear sphericity and HME-I cellular sphericity between the three conditions **D,F:** Bar graph showing the fraction of nuclei/cells

respectively that have sphericity values lesser than a particular threshold value **G:** bar graph showing the HMF nuclear aspect ratio when embedded as a singlets vs as an aggregate (HMF-S and HMF-C respectively) (graph and analysis: C,D: N=3, n~600; E,F: N=2 n~800, G: N=2, n~200 Mean +/- SEM ****P<0.0001, ns- non-significant). **H:** violin plot showing the HME-I cellular and the HMF3A nuclear orientations in the three different conditions in three different fields of view. “F”: fibroblast, “E”: epithelial ; “F1”,”E1” represents the fibroblasts nuclei and epithelial cells of field 1 respectively (graph: the width of the violin qualitatively represents the frequency of that observation, midline represents median with first and the third quartile).

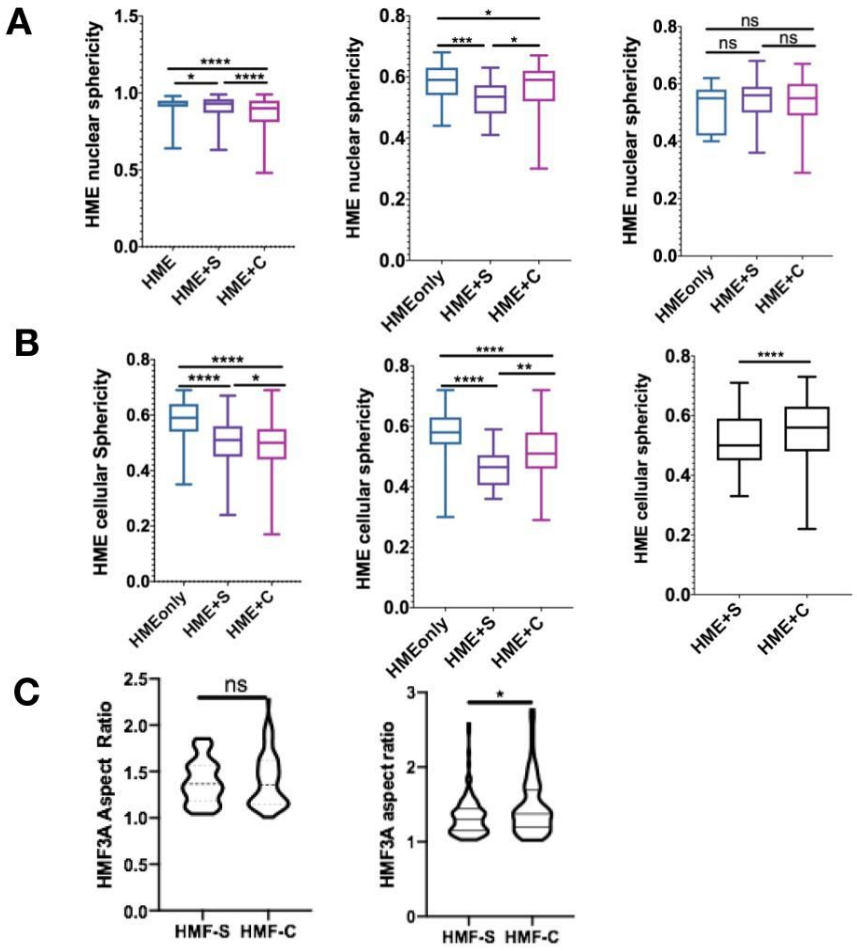

Figure 3.5S: **Replicate data for Figure 3.5(C,D,E)**: **A,B**: Box plot showing the HME-I nuclear and cellular sphericity respectively between conditions in three different replicates (graph: midline: Median, error bar: minimum and maximum values) **C:** Violin Plot showing the aspect ratio of HMF3A as singlet and when embedded as clumps in 3D collagen gel. (graph: the width of the violin qualitatively represents the frequency of that observation, midline represents median with first and the third quartile). Analysis A: n~200 B: n~400 C: n~100; mann whitney t-test : ns-non-significant, ****P<0.0001, **P<0.01, *P<0.05.

As proposed in our hypothesis, we wanted to check if such pulling of epithelial cells by fibroblasts through the collagen matrix induces DNA damage in the nuclei of the epithelial cells under mechanical stress. We stained the samples for gH2Ax (*Figure 3.6A*) and measured the number of foci in the HME-I nuclei in each case.

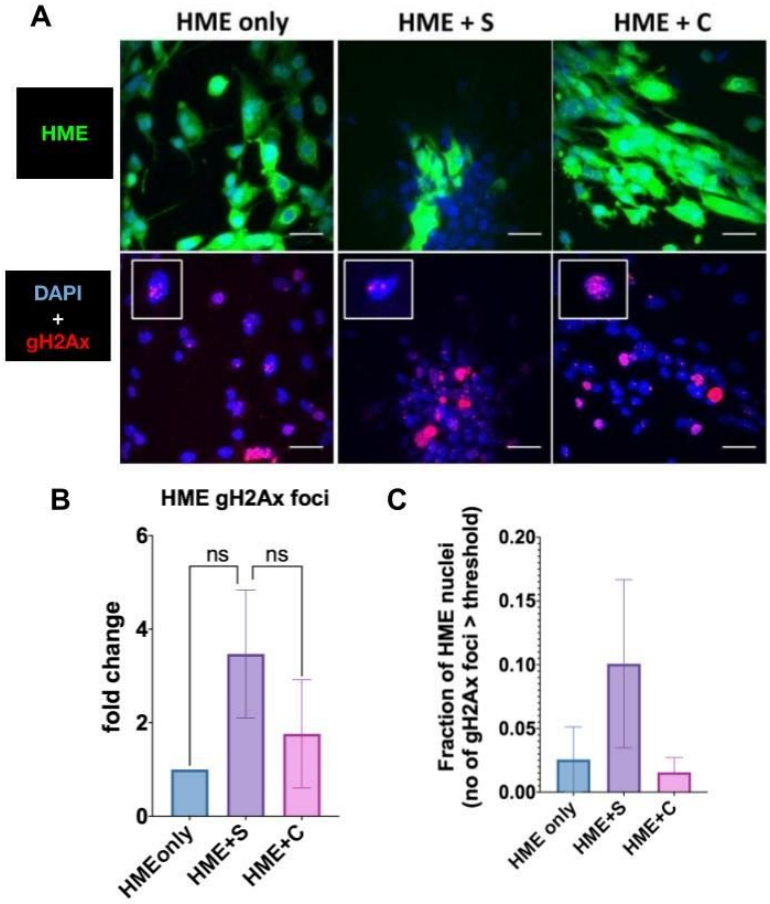

Figure 3.6: **DNA damage in epithelial cells when co-cultured with fibroblasts: A:** Representative micrographs of **(above)** 3D co-culture of HME-I with singlets and aggregates of HMF3A (centre: HME + S and right: HME + C respectively) with HME-I monoculture as control (HME only) and (below) immunostained for gH2Ax to measure DNA damage (Scale Bar = 50 μm) **B:** Plot showing the Average fold change in gH2Ax foci between the three conditions in HME-I nuclei from two different replicate.**C:** Bar graph showing comparing the fraction of HME-I cells in three conditions that have gH2Ax foci numbers greater than a threshold number. (graph and statistics: A,B: N=2, n~400, Mean +/- SEM, multiple t-test ns-non-significant, *P<0.05).

As explained earlier, the average values showed a significant increase in presence of singlets whereas dropped in the presence of clumps, this could be because larger number of contacts are made between HME-I and HMF3A when HMF3A is incubated as singlets than as clumps The average elongation and gH2Ax might be higher in case of HME +S for this reason. Comparing the fraction of nuclei having gH2Ax foci above threshold numbers in each condition for two different replicates, we noticed that the higher fraction of cells have higher gH2Ax foci number in HME + S as compared to HME+C and HME control (*Figure 3.6B*). When compared replicate-wise, we see the maximum gH2Ax foci numbers are higher for HME+C as compared to HME+S indicating that the efficiency of the contacts made between HME-I and HMF3A in the two conditions may play a role. In HME+S since fibroblasts are embedded throughout the gel, the efficiency of contact making could be higher than HME + C where fibroblasts clump are incubated close to HME-I clumps and the contacts could be lesser.

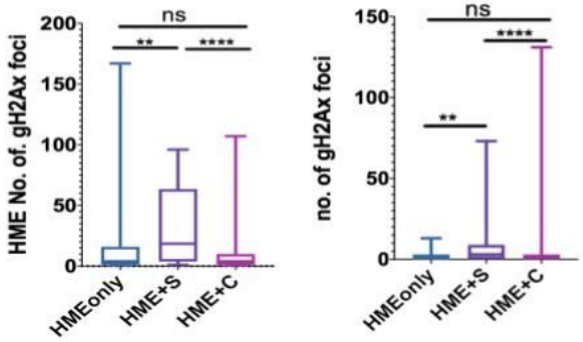

Figure 3.6S: **Replicate data for figure 3.6(B):** Box plot showing the No of gH2Ax foci in HME nuclei in the three different conditions for two biological replicates (graph and analysis: n=200, Midline: Median, error bar: minimum and maximum values, students' t-test, ****P<0.0001, **P<0.01, ns- non significant)

This observation was interesting to us because fibroblasts are known to be recruited and aggregated at the site of wound, where they come in contact with epithelial cells. This could potentially induce mechanical stress and DNA damage on the epithelial cell

nuclei, predisposing it to become tumorigenic.

3.2.2 Collagen remodelling happens during fibroblast driven HME cell migration

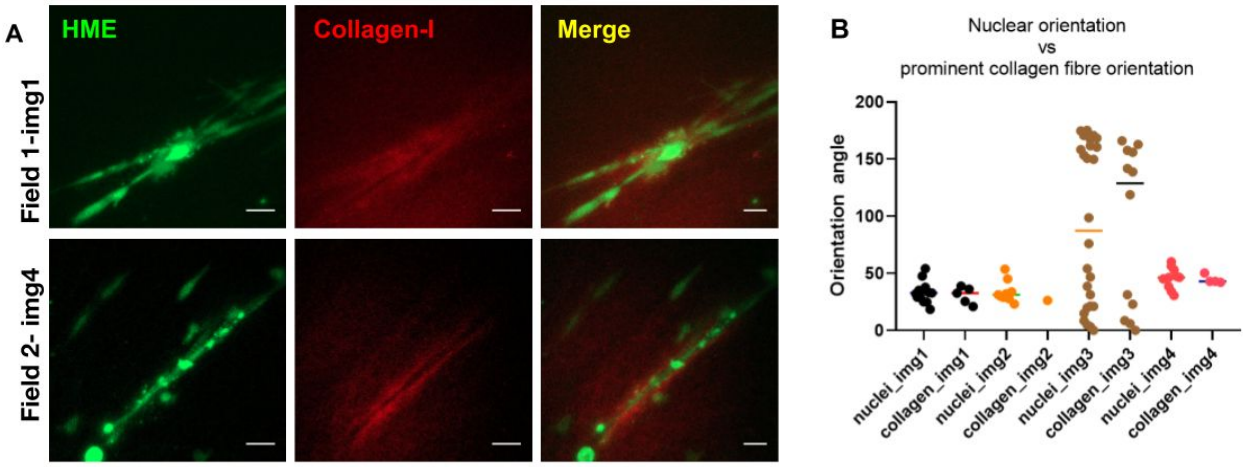

Figure 3.7: **Collagen-I matrix remodelling in HME+C**: **A**: Representative images of two fields of a HME+C sample (centre) immunostained for collagen-I and (left) HME-I marked with green cytotracker (Scale Bar: 50 μm). **B**: Scatter plot of the orientation angles of HME-I cells prominent collagen-I trail in their corresponding field of view in four different fields.

In order to check the matrix remodelling associated with fibroblast driven migration of HME-I cells, we stained a co-culture sample of HME+C for collagen-I and imaged four different fields of view (*Figure 3.7A*). We observed that the orientation of the most visible collagen fibres in a field of view is similar to the orientation angles of elongated HME-I nuclei in the same field of view (*Figure 3.7B*). In case of non-elongated nuclei, we observe no specific collagen fibre orientation around them, as evident from the images. We have quantified the orientation angles in four separate fields of view. But it is yet to be understood in full detail what is causing such trails of collagen. Whether this is an effect of the HME being pulled through the matrix, or if its the trail left by fibroblasts that have already travelled through the matrix or are these collagen deposition by fibroblasts is yet to be elucidated.

3.3 Showing higher elongation in epithelial cells when co-cultured with more contractile fibroblasts .

3.3.1 Higher HME-I elongation is observed when co-cultured with more contractile fibroblasts

As mentioned earlier, the fibroblasts that aggregate at the site of the wound are known to become more contractile due to biochemical signalling associated with the wound environment. In order to study the role of fibroblast contractility in determining mechanical interaction between fibroblasts and epithelial cell, we compared HME-I nuclear and cellular features in three different condition: HME-I clump control (HMEonly), HME-I co-cultured with clump of normal HMF3A fibroblasts (HME+C) and HME-I co-cultured with PR spheroids of HMF3A (HME + PR) all embedded in 3D collagen-I matrix for two days (*Figure 3.8A,B*).

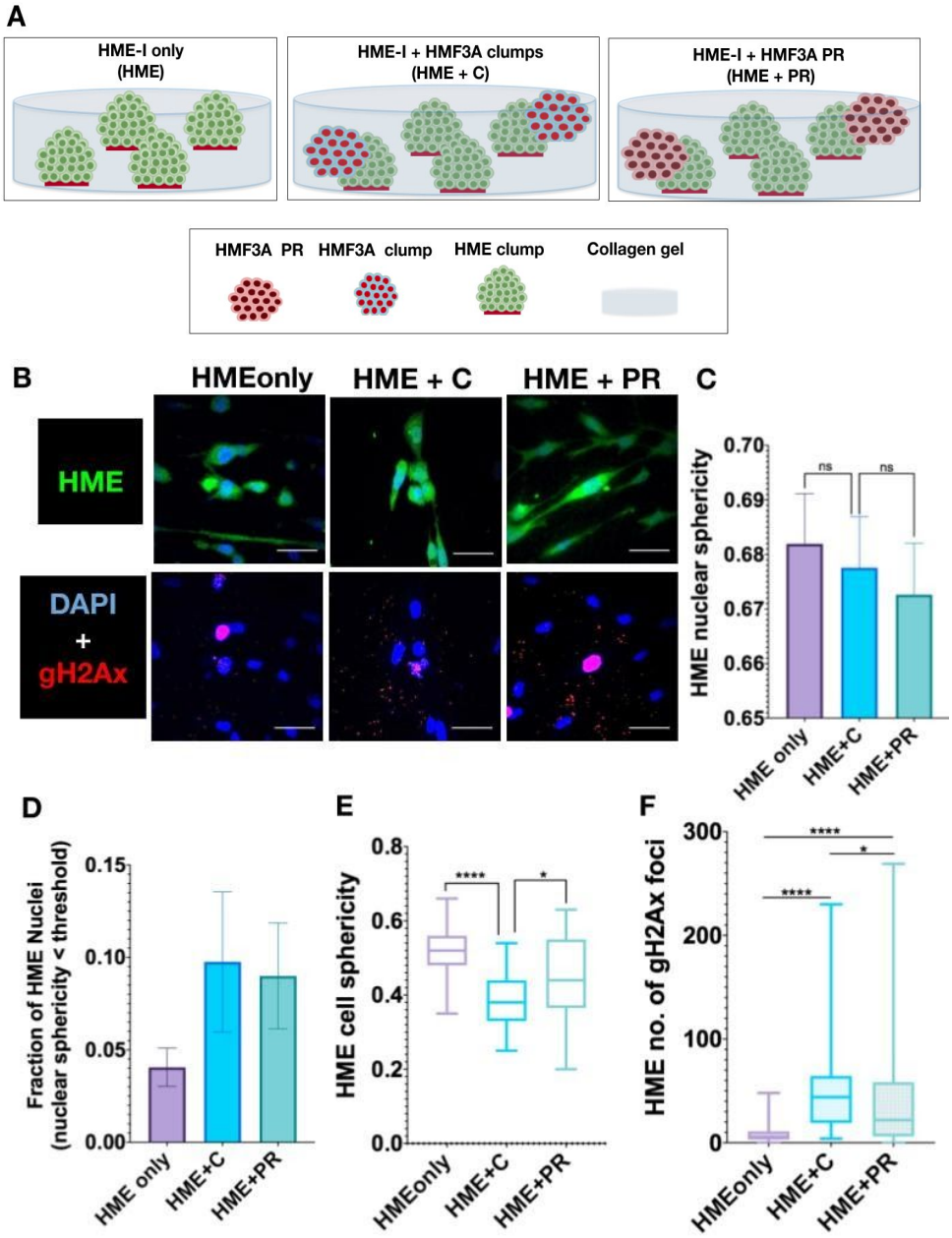

Figure 3.8: **Effect of pulling by more contractile vs less contractile fibroblasts: A:** Schematic of the different conditions in the experiment. **B:** (Above) Representative micrographs of HME-I clump (Left: HME), HME-I co-culture with clumps of HMF3A, (Centre: HME+C) and HME-I co-culture with PR spheroids of HMF3A (Right: HME+PR) after embedding in 3D collagen-I matrix for two days (Scale Bar = 50um), (Below) Representative micrographs of DNA (DAPI) and gH2Ax immunostaining in the corresponding field of view of the above mentioned samples (Scale Bar: 50 μm). **C:** Bar graph comparing

the HME-I nuclear sphericity between the three conditions **D:** Bar graph comparing the fraction of HME-I nuclei that have sphericity values lesser than a particular threshold value in HMEonly, HME+S, HME+C **E:** Box Plot showing the the HME-I cellular sphericity values between the conditions in one replicate HME nuclear number of gH2Ax foci between the three conditions (graph and analysis: C,D: N=3, n~600 Mean +/- SEM multiple t-test, ns-non significant; E: N=1, n~20 F: N=1, n~ 200 E,F: Median, error bar represents minimum and maximum values mann whitney t-test, ****P<0.0001, *P<0.05).

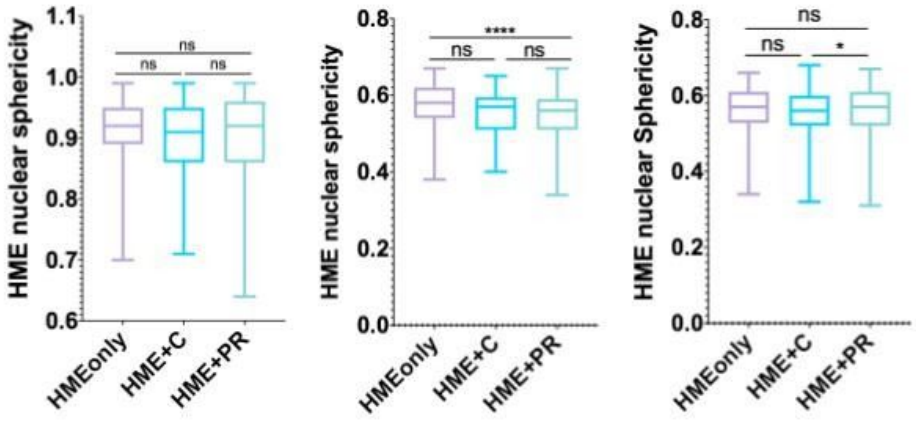

Figure 3.8S: **Replicate data of Figure 3.6(C):** Bar graph of HME-I nuclear sphericity in the three different conditions in three biological replicates. (Graph and analysis n~200, Midline: Median, error bar: minimum and maximum values, students' t-test, ****P<0.0001, *P<0.05, ns- non significant)

We observed that the average nuclear sphericity is higher in HMEonly than HME+C and further lower in HME+ PR(*Figure 3.8C*). The fraction of elongated HME-I nuclei (sphericity lesser than a threshold value) seems to be the highest in the case of the co-culture systems as compared to control and higher in HME+C as compared to HME+PR (*Figure 3.8D*). Although the latter observation seems contrary to our hypothesis, when looked at each replicate we observed that the minimum nuclear sphericity is still lower in HME+PR as compared to HME+C. This validates our hypothesis to an extent. We are still yet to investigate the exact mechanical factors that cause a more contractile fibroblast to increase nuclear elongation in HME-I. The higher HME-I elongation by more contractile fibroblasts, we suspect, can be explained by the marked increase in motility of more contractile fibroblasts which might hence pull the

HME-I it makes contact with more efficiently. Another possibility is that these fibroblasts could in-turn remodel the collagen matrix that it moves through pulling the matrix to orient in the direction of its movement. This will in turn lead to the elongation of HME-I located proximal to the remodelled matrix to orient in the same direction i.e. along axis of fibroblast movement. A more contractile fibroblast may exert a larger force on its surrounding matrix, which further adds to the chances of this phenomenon.

To see if the nuclear elongation translates to increased DNA damage, we compared the number of gH2Ax foci in the HME-I nuclei in the three different conditions and observed, as expected, that the gH2Ax foci in the HME-I nuclei is higher in the case of HME+PR as compared to HME+C and further lower in HMEonly (*Figure 3.8F*). But this observation remains restricted to one replicate.

If a more contractile fibroblast is indeed able to exert a larger force to pull epithelial cells, and cause more DNA damage in them, this could add to the multitude of mechanisms that initiate tumours. This could also explain the neoplastic transformation of cells from OSE that get locked in the extracellular matrix of the ovarian tissue during the post ovulatory repair process, that was discussed earlier, in the introduction.

5

CONCLUSION AND FUTURE DIRECTIONS

There seem to be a multitude of mechanical interactions in wound-like scenarios which may predispose otherwise normal epithelial cells to become tumorigenic by inducing genomic instability through mechanical stress induced DNA damage. During the course of my masters' thesis, we successfully developed a 3D co-culture model to study mechanical interactions between fibroblasts and epithelial cells. This model could also be used to study interactions between multiple types of cells in 3D growth conditions mimicking physiological systems. We established the pulling effect of fibroblasts on epithelial cells using HMF3A and HME-I respectively, thereby trying to keep the question relevant to interactions in mammary tissues. Further, we showed that more contractile fibroblasts and aggregate of fibroblasts elongate the nuclei of the epithelial cells more than their controls. The DNA damage in the epithelial nuclei incurred in such conditions is also higher. We showed that there is definitely matrix remodelling around elongated epithelial cells. But what remains to be investigated with respect to our hypothesis is whether fibroblasts induced migration of epithelial cells through denser or stiffer matrices could lead to more DNA damage than in matrices of lesser density. We have thus hinted at a role of physical and mechanical interactions in wounds that could possibly initiate epithelial cell tumor. Yet there is still more investigation that needs to be done to be sure of the kind of mechanical interaction between fibroblasts and epithelial cells that facilitate such elongation in the epithelial cells. Complex systems that facilitate a lot of such interactions can be designed in order to tap the rare event of tumour initiation. In conclusion, there seems to be a light at the end of the tunnel, but we are still at its beginning.

6

REFERENCES

1. Arnold, K.M., Opdenaker, L.M., Flynn, D., and Sims-Mourtada, J. (2015). Wound healing and cancer stem cells: inflammation as a driver of treatment resistance in breast cancer. Cancer Growth Metastasis *8*, 1–13.
2. Attieh, Y., Clark, A.G., Grass, C., Richon, S., Pocard, M., Mariani, P., Elkhatib, N., Betz, T., Gurchenkov, B., and Vignjevic, D.M. (2017). Cancer-associated fibroblasts lead tumor invasion through integrin-β3–dependent fibronectin assembly. The Journal of Cell Biology *216*, 3509–3520.
3. Foster, D.S., Jones, R.E., Ransom, R.C., Longaker, M.T., and Norton, J.A. (2018). The evolving relationship of wound healing and tumor stroma. JCI Insight *3*.
4. Frank, S.A. (2007). Stem Cells: Tissue Renewal. In Dynamics of Cancer: Incidence, Inheritance, and Evolution, (Princeton University Press),.
5. Irianto, J., Xia, Y., Pfeifer, C.R., Athirasala, A., Ji, J., Alvey, C., Tewari, M., Bennett, R.R., Harding, S.M., Liu, A.J., et al. (2017). DNA Damage Follows Repair Factor Depletion and Portends Genome Variation in Cancer Cells after Pore Migration. Curr. Biol. *27*, 210–223.
6. Labernadie, A., Kato, T., Brugués, A., Serra-Picamal, X., Derzsi, S., Arwert, E., Weston, A., González-Tarragó, V., Elosegui-Artola, A., Albertazzi, L., et al. (2017). A mechanically active heterotypic E-cadherin/N-cadherin adhesion enables fibroblasts to drive cancer cell invasion. Nat. Cell Biol. *19*, 224–237.
7. Murdoch, W.J., Townsend, R.S., and McDonnel, A.C. (2001). Ovulation-Induced DNA Damage in Ovarian Surface Epithelial Cells of Ewes: Prospective Regulatory Mechanisms of Repair/Survival and Apoptosis. Biol. Reprod. *65*, 1417–1424.
8. Nicholas B Berry, S.A.B. (2008). Ovarian cancer plasticity and epigenomics in

the acquisition of a stem-like phenotype. J. Ovarian Res. *1*, 8.

9. Ondeck, M.G., Kumar, A., Placone, J.K., Plunkett, C.M., Matte, B.F., Wong, K.C., Fattet, L., Yang, J., and Engler, A.J. (2019). Dynamically stiffened matrix promotes malignant transformation of mammary epithelial cells via collective mechanical signaling. Proc. Natl. Acad. Sci. U. S. A. *116*, 3502–3507.
10. Pfeifer, C.R., Alvey, C.M., Irianto, J., and Discher, D.E. (2017). Genome variation across cancers scales with tissue stiffness – an invasion-mutation mechanism and implications for immune cell infiltration. Current Opinion in Systems Biology *2*, 103.
11. Roy, B., Venkatachalapathy, S., Ratna, P., Wang, Y., Jokhun, D.S., Nagarajan, M., and Shivashankar, G.V. (2018). Laterally confined growth of cells induces nuclear reprogramming in the absence of exogenous biochemical factors. Proc. Natl. Acad. Sci. U. S. A. *115*, E4741–E4750.
12. Peter Kujath, A.M. (2008). Wounds – From Physiology to Wound Dressing. Deutsches Ärzteblatt International *105*, 239.
13. Hanahan, D., and Weinberg, R.A. (2000). The Hallmarks of Cancer. Cell *100*, 57–70.
14. Hanahan, D., and Weinberg, R.A. (2011). Hallmarks of Cancer: The Next Generation. Cell *144*, 646–674.